A TACTICAL GPS GUIDANCE SYSTEM

D. L. Gieseking, Senior Staff
H. L. Engel, Senior Scientist
Hughes Aircraft Company
Missile Systems Group
Canoga Park, CA

V. Calbi, Director of Systems Engineering GPS
A. J. Van Dierendonck, Consultant
Magnavox
Advanced Products Division
Torrance, CA

ABSTRACT

The paper presents results of a design study that defined an optimal (cost vs performance) guidance system that uses the NAVSTAR system. The paper will describe the trades that led to the system configuration. A sequencing receiver (receiver that listens to one satellite at a time) was chosen. This required the navigation system to position the code and frequency of the receiver tracking loops where the receiver switches satellites. Receiver measurements are processed in a U-D formulation of a Kalman filter to update the navigation equations to perform in-flight alignment and parameter estimation of the strapdown gyro biases. Receiver and guidance system performance are presented.

INTRODUCTION

The NAVSTAR Global Positioning System (GPS) is a highly attractive system for the guidance of tactical missiles. Being a satellite-based navigation system, it provides world-wide coverage, is terrain independent, and operates in all weather — day or night. In addition, the system may be used by any number of missiles and the missiles need not radiate. A guidance system that is highly resistant to ECM (electronic countermeasures) can be designed by combining an inertial subsystem with a GPS receiver.

The Air Force Armament Laboratory is sponsoring a competitive development of a Tactical Global Positioning System Guidance (TGPSG) system with the purpose of developing a low-cost, jam resistant guidance system. The primary purpose of this program is to develop a midcourse guidance system with a secondary objective of “GPS all-the-way”, i.e., midcourse and terminal guidance.

This paper presents the results of the design study conducted by Hughes Aircraft Company and Magnavox-Advanced Products Division (subcontractor for receiver development) which defined their TGPSG system.

TGPSG SYSTEM DESCRIPTION

The elements of the TGPSG system are shown in block diagram form in Figure 1. The Guidance Processor (GP) maintains an inertial reference using data provided by the Low Cost Inertial Guidance System (LCIGS). Position and velocity computed using this inertial reference will be in error because of biases and inaccuracies in the strapdown inertial measurement instruments. To correct this long-term error, the GP incorporates measurement data from the class M GPS receiver (M-receiver) from which position and velocity information can be derived. An upper-diagonal (U-D) form of a Kalman filter is used to derive position, velocity, and tilt corrections for inertial reference, to estimate gyro biases and to improve the estimates of clock time and frequency. The GP also provides rate-aiding information to the M-receiver. This aiding information allows the receiver to track the GPS satellite signals with narrower bandwidths than would normally be employed if the receiver tracking loops were forced to track throughout the entire range of vehicle dynamics. As a result, the receiver can track the satellite signals at higher jamming-to-signal power ratio (J/S) conditions. The accuracy with which aiding can be provided ultimately determines the minimum tracking bandwidth and, therefore, the maximum J/S ratio.

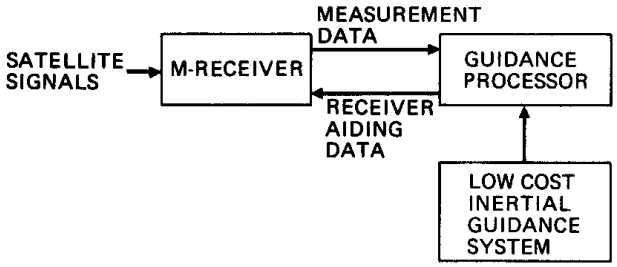

Fig. 1. Tactical GPS guidance system block diagram

M-RECEIVER DESCRIPTION

The essential features of the M-receiver are shown in a functional block diagram in Figure 2. The receiver utilizes two tracking loops, a delay-lock loop for tracking the pseudorandom code transmitted by the satellite, and a Costas or automatic frequency control (AFC) loop for tracking the doppler-shifted carrier. Pseudorange data is obtained from the code tracking loop, and is used for determination of position. Pseudodelta-range data, which is proportional to doppler, is used in the filter as an independent velocity measurement. The code and carrier loops mutually aid each other. The satellite signal is a phase-shift keyed (PSK) signal. The phase shifting must be removed by the code loop so that the carrier tracking loop can track the carrier. The carrier loop, in turn, provides the frequency of the carrier to drive the pseudorandom code generator. By employing a higher-order, wide-bandwidth carrier loop to track the dynamics of the vehicle, a first order code

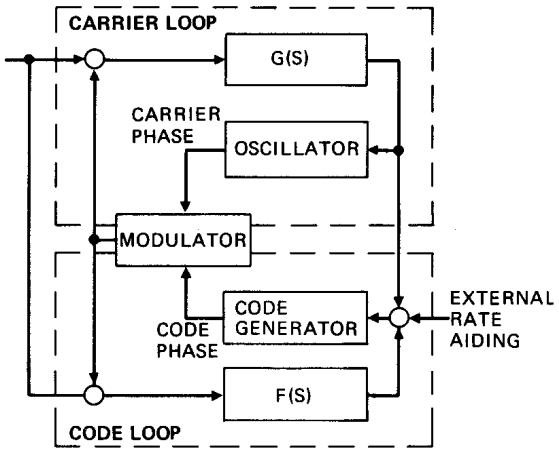

Fig. 2. M- receiver functional block diagram

is adequate to generate code phase. A sequential receiver design (tracks one satellite at a time) was a chosen for the M-receiver to minimize cost while still providing high ECM resistance.

The receiver has three tracking modes and automatically enters the highest accuracy mode possible given the carrier-to-noise ratio (C/N) existing in the receiver at that time. The three modes in order to descending accuracy are: 1) Costas and code track, 2) AFC and code track, and 3) code-only track. In modes 1 and 2, the receiver provides both pseudorange and pseudodelta-range measurements. In mode 3, only pseudorange measurements are provided. When the receiver is in mode 3 tracking, the code loop also uses the correlator from the carrier loop to measure simultaneous early-late (E/L) power in the code loop, to maximize antijam (AJ) capability. In mode 3, the receiver must receive rate-aiding information from the GP to replace the frequency information no longer available from the carrier loop. The accuracy with which this aiding information can be provided is the dominating factor in determining the maximum AJ capability of the receiver.

In addition to the three tracking modes, the receiver has an acquisition mode and two reacquisition modes. In the acquisition or reacquisition mode, the receiver reconfigures itself to function in the manner indicated in Figure 3. The receiver receives pseudorange and pseudorange-rate estimates from the GP and uses this information to establish the search pattern for the receiver. The search pattern discriminates against multipath by searching from the short side because the shortest pseudorange is the direct signal.

GUIDANCE PROCESSOR (GP) DESCRIPTION

The functions currently planned to be performed in the GP are shown in Figure 4. The primary functions are inertial navigation, filtering, to provide corrections to the navigation

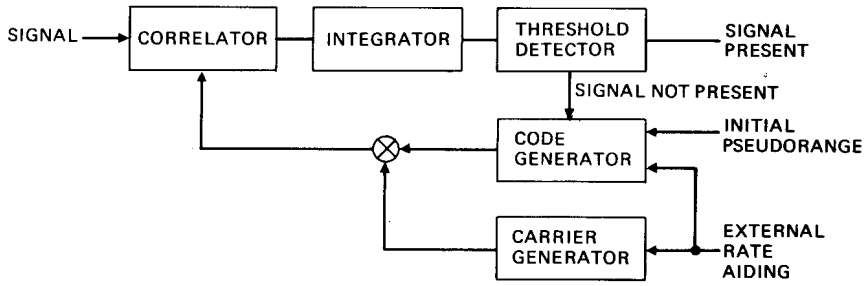

Fig. 3. Acquisition and reacquisition functional block diagram

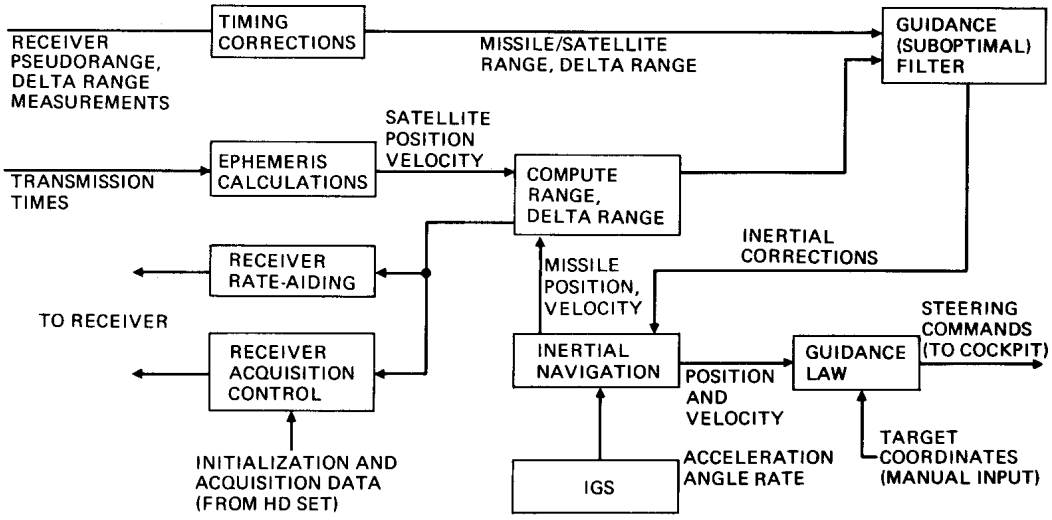

Fig. 4. Guidance processor functional block diagram

equations, and rate aiding of the receiver. Inertial navigation is performed using a north-reference set of navigation equations which computes latitude, longitude, and altitude from measured accelerations. For the flight test program, these accelerations are referenced to a set of platform axes and error terms are added to the measurement to simulate LCIGS. Thus, the performance of the navigation equations is typical of the performance that would be experienced if the LCIGS were being used for inertial measurements.

A U-D (upper-diagonal) formulation of the Kalman filter is used to process receiver measurements and to derive corrections for the navigation equations. Since the filter is recursive, it handles the sequential measurements very naturally; in fact, even though the pseudorange and pseudodelta-range measurements for a given satellite are available simultaneously, they are processed sequentially in the filter. A 14-state filter is used to compute three positions, three velocities, clock phase, clock frequency, three tilts and three gyro biases.

In a sequential receiver, two forms of receiver aiding are required. When the receiver sequences from one satellite to the next, the GP must supply an estimate of the

pseudorange accurate enough so the receiver need not search and can immediately start tracking the new satellite. The GP must also supply an estimate of pseudorange rate to aid the carrier loop in rapid acquisition on the carrier. These estimates are known as preposition information. The second form of aiding is required on mode 3, the GP must continually supply pseudorange rate information to reduce the dynamics that the code loop must track.

INERTIAL GUIDANCE SYSTEM DESCRIPTION

The TGPSG system is designed to work with the LCIGS currently being developed by the Air Force. LCIGS is a strapdown inertial measurement unit with three single degree-of-freedom gyros and three accelerometers. Since the LCIGS system is still in the design phase, performance was computed for a range of accelerometer biases. This parameter was chosen for variation because it is not being estimated in the filter. The gyro biases are being estimated in the filter and as long as these quantities can be estimated to the level shown, changes in the instrument quality will not affect system performance.

DESIGN TRADE STUDIES

A series of design trade studies were conducted in order to define the M-receiver. The purpose of these studies was to reduce the system cost while retaining, or enhancing, system jam resistance. A previous study conducted by Hughes Aircraft Company for the Air Force identified a number of techniques for reducing system cost.

LAUNCH AIRCRAFT INTERFACE

One such technique was the use of the launch aircraft high dynamic receiver, an inertially aided receiver, to initialize the M-receiver. The concept is to eliminate functions from the missile receiver that can be performed in the launch aircraft receiver and provided to the missile over the aircraft-to-missile interface. Data that can be provided from the high dynamics receiver includes; the satellite constellation being tracked, the satellite ephemerides, satellite clock data, time, measured pseudorange, measured pseudodelta-range, and an ionospheric correction.

These data allow elimination of the following functions from the M-receiver: 1) the C/A acquisition code, because the data allows direct acquisition of the P-code; 2) data demodulation and a satellite almanac, because the satellite data is being supplied over the interface and 3) the L_2 frequency, because the ionospheric correction is provided. The last function is very significant because it greatly simplifies the RF portion of the receiver.

In addition to the data supplied by the launch aircraft discussed above, the aircraft interface could supply satellite signals to the missile receiver. This would require an RF cable from the aircraft antenna to the missile pylon, but it would allow the missile to acquire the satellite signals prior to launch providing a “lock-on-before launch” capability.

Another technique involves simplification of the receiver by using information from the inertial navigation solution maintained in the guidance processor. Integration of the inertial guidance system into the TGPSG system provides the system with significantly improved jam resistance and reliability as an alternate guidance source. The inertial information allows one to consider sequential receiver designs that rely on aiding from the inertial system in order to track. A priori, it was felt that a sequential receiver, a receiver that tracks one satellite at a time for an extended period of time, would provide the optimum receiver design on a cost /performance basis. The potential cost savings are obvious; elimination of three carrier tracking loops, factor of three to four reduction in computer throughput in the guidance processor and the receiver process controller, elimination of 3 codes and elimination of 3 or 4 correlators. Figure 5 shows the potential hardware saving of the sequential M-receiver compared to a high dynamic receiver.

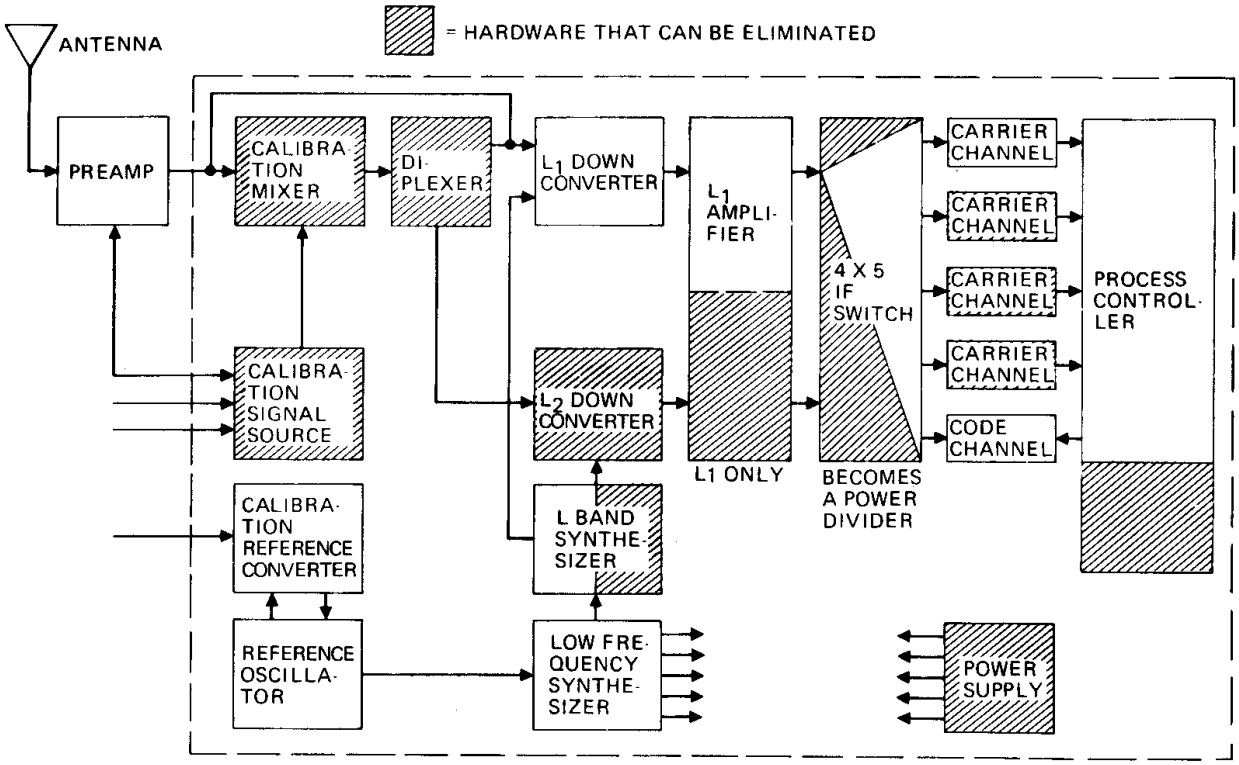

Fig. 5. M-receiver hardware simplifications

RECEIVER CONFIGURATION

Two parallel studies were undertaken to define the system configuration; one, to determine performance of various receiver options given a level of aiding accuracy and two, to determine the effect of the receiver options on aiding accuracy. Three generic receiver forms were studied; sequential, continuous four-channel, pseudo four-channel. A pseudo four-channel receiver is a sequential receiver that rapidly sequences through the four satellites and maintains four simultaneous code tracking loops. Within each form, there are addition trades involving the number of coders and correlators used to mechanize the tracking loops. Only three configurations will be reported on herein as they bound cost and performance and include the chosen design. These three configurations are:

1. Four coders/five correlators (as in the high dynamics set)

2. One coder/two correlators

3. One coder/one correlator

SEQUENTIAL RECEIVER

The choice of sequencing rate in a one coder sequential receiver is driven by conflicting requirements. The maximum sequencing rate is limited by the length of time required to declare that the signal is present and the minimum sequencing rate by the ability of the guidance processor to preposition the code when sequencing to another satellite. Since a ±1/2 chip early/late sampling code loop is only linear over ±1/2 chip, it is highly desirable that the code be prepositioned at least that accurately most of the time. This requires that the aiding accuracy along the line-of-sight be better than 0.025 chips/sec (2.5 ft sec) for a satellite sequencing rate of 1/6 Hz. Typical RSS inertial aiding errors were computed using a covariance analysis program for a range of measurement intervals assuming four simultaneous measurements each interval (Figure 6). It was felt that a sequencing receiver at 6 seconds per measurement would give velocity errors similar to the 12 sec data rate curve shown. This is adequate to supply the prepositioning data. Since the receiver is able to provide a reliable data present indication at this rate and since the processor has adequate throughput to incorporate the measurements, 1/6 Hz was chosen for the sequencing rate. As fast a sequencing rate as practical was considered most desirable to improve navigation accuracy. Concern over approximations in the covariance analysis also affected this decision.

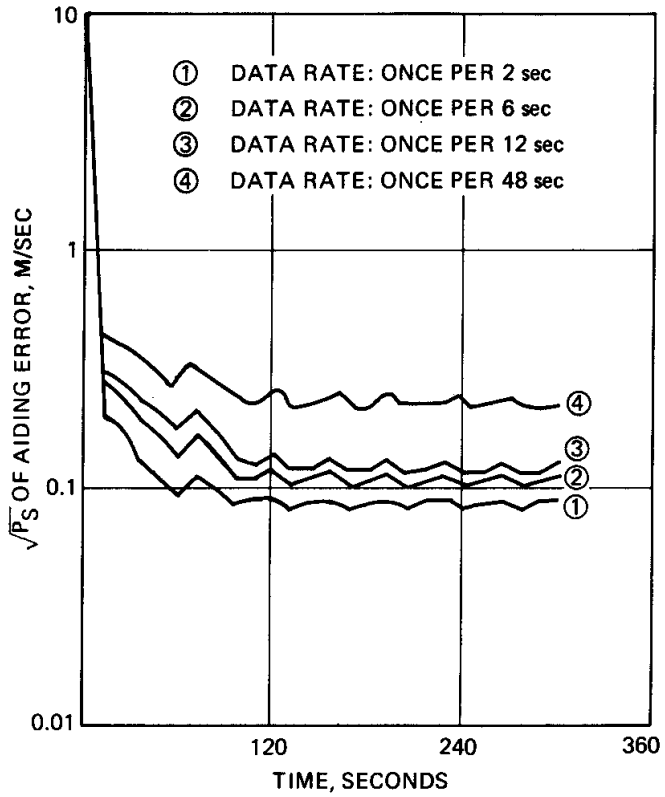

Fig. 6. Inertial aiding error

PSEUDO FOUR- CHANNEL RECEIVER

Since the pseudo four-channel receiver continuously maintains four code tracking loops, it is desirable to sequence through the satellites as rapidly as possible. The maximum sequencing rate is limited by the IF bandwidth and hardware constraints, e. g., code generator slew rate. Assuming the ability to instantaneously slew to a new code, a pseudo four-channel sequencing rate of 12.5 Hz was selected for a receiver with two correlators for simultaneous early/late power measurements. For a receiver with one correlator that τ-dithers to make early/late power measurements, a sequencing rate of 6.25 Hz was selected.

FOUR-CHANNEL RECEIVER

The four- channel receiver that was analyzed was functionally identical to the Magnavox high dynamics receiver and uses four code generators and five correlators. However, the bandwidths were optimized to maximize the J/S capability of the receiver in the missile environment. At low J/S (jam/signal) ratio, the receiver mechanizes four carrier tracking loops and time shares one code loop. At high J/S, the receiver mechanizes four continuous tracking code loops with the correlators being τ-dithered to provide early/late power measurement.

COMPARISON

A comparative ranking of the performance and cost of the receiver designs relative to a sequential receiver with one coder and two correlators is shown in Table 1. Each receiver has been optimized for the minimum loop bandwidth and for the optimum loop order for that design. Two columns of relative AJ are shown and they differ by the relative aiding capability assumed. The unequal aiding column is probably most appropriate for design because the four-channel designs will provide more accurate navigation. However, as will be seen, navigation accuracy is not the only factor affecting aiding accuracy. The sequential (1 coder/2 correlator) design was selected for the M-receiver over the four-channel on the basis that the modest performance improvement was not worth the cost. When compared to the sequential (1 coder/l correlator) design the performance improvement was felt to justify the cost. The pseudo four-channel designs were eliminated on the basis of design risk. Clearly with today's technology, the assumption of instantaneous code slewing is unjustified and the design would suffer a cost and/or performance penalty as a result.

Table 1

		Relative AJ (Equal Aiding)	Relative AJ (Unequal Aiding)	Relative Cost
Sequential	1 coder 1 correlator	-1.5 dB	-1.5 dB	0.85
	1 coder 2 correlators	0.0 dB	0.0 dB	1.0
Pseudo four-channel	1 coder 1 correlator	-3.0 dB	-1.5 dB	0.85
	1 coder 2 correlators	-1.5 dB	0.0 dB	1.0
Four-channel	4 coders 5 correlators	0.25 dB	1.75 dB	2.0

RATE AIDING LIMITATIONS

The ability to accurately provide aiding information to the code tracking loop is vital to the ultimate AJ capability of the receiver. Phase velocity and acceleration caused by vehicle dynamics determine the tracking loop bandwidth. The signal time rate-of-change can be effectively reduced by supplying phase velocity (pseudorange-rate) information corrected with phase acceleration to the tracking loop.

The ability to provide accurate rate aiding is limited by a number of factors; namely, navigation accuracy, computational delays in supplying aiding and clock g-sensitivity. Only navigation accuracy is a function of receiver measurement rate. The other error sources were analyzed to determine their approximate effects because they form a bound that limits the minimum receiver bandwidth. The Air Force specified the set of vehicle dynamics shown in Table 2. Given the throughput of the guidance processor, it was estimated that the time required to perform the aiding computations would be 35 msec. At the specified vehicle acceleration, the velocity error would be

$$\Delta V = aT_c = 1.\ 75 \text{ m/sec} \qquad (1)$$

This magnitude of velocity error would limit the receiver to unacceptable large tracking bandwidths. It was desired to reduce this error by an order of magnitude to the level of the aiding error determined from the covariance analysis data shown earlier. A flight computer capable of that throughput was not available. However, since acceleration at the measurement time is available, the aiding computation can be extrapolated by the computational delay time. Then the dynamic error can be reduced to the change in acceleration (jerk) over the extrapolation time. This error is only

$$\Delta V = 1/2JT_c^2 = 0.06 \text{ m/sec} \qquad (2)$$

which is less than the predicted navigation velocity errors.

Since the antenna and the inertial measurement unit are usually not co-located, angular accelerations will cause a velocity error. In most missile systems, this error source can be neglected because the lever arms are short and high angular acceleration exist only for short periods of time. Thus, the velocity error introduced will appear as a noise source rather than a long term velocity offset to the tracking loops.

Table 2. Vehicle dynamics

Parameter	Measurement
Velocity	0-900 m/sec (max)
Acceleration	50 m/sec^2 (max)
Jerk	100 m/sec^3
Pitch	Any
Pitch rate	100 deg/sec
Pitch angular acceleration	85 deg/sec^2
Yaw	Any
Yaw rate	100 deg/sec
Yaw angular acceleration	100 deg/sec^2
Roll	Any
Roll rate	270 deg/sec
Roll angular acceleration	500 deg/sec^2

The crystal clock used as a basic frequency reference for the M-receiver is also a source of aiding errors. The most troublesome clock error source is acceleration sensitivity While the clock is under acceleration, the output frequency can be shifted by 1 part in 10^{+9} or 10^{+10} per/g. The particular clock chosen and its mounting relative to the g vector will determine which scale factor is most appropriate. If the scale factor is 10^{-10}/g, a 5 g acceleration will cause an aiding error of approximately 0.15 m/sec. This is on the order of the aiding error due to dynamics. However, at the high end of the scale, the error source would become a dominating, and limiting factor.

SEQUENTIAL RECEIVER ANALYSIS

A sequencing receiver was designed utilizing a single RF channel with one PN code generator. Analysis was performed to determine the benefit of implementing aided carrier tracking, determining the best order of the tracking loops and the optimum bandwidths.

CARRIER TRACKING - UNAIDED AND AIDED

At higher signal-to-noise conditions, unaided carrier tracking (not aided with IGS) is of benefit for providing measurements for IGS alignment. It also provides a backup capability during the test program that can be used for system fault isolation, in event of integrated IGS M-receiver difficulties.

The benefit of using IGS aiding in the carrier tracking loop occurs primarily when the IG aiding accuracies are insufficient or are marginal for direct code loop aiding. In this case

the aided carrier loop output is used to aid the code loop. The benefit decreases as the IGS accuracies become better because the IGS becomes more accurate than the aided carrier loop output, since the carrier loop output is corrupted with filtered jamming noise.

TRACKING LOOP ORDER

For any receiver, an increase in the order of a tracking loop increases the receiver's capability to track in the presence of higher order aiding errors (velocity, acceleration, jerk, etc.) In the case of a sequential receiver, however, that capability must be traded against its transient error characteristics. Of course, those characteristics are dependent on the bandwidth of the loop, which is primarily specified by the J/S capability.

To obtain a bound on the bandwidth, we use the relationship

$$\sigma_N^2 = \frac{B_L}{NS/N_o}\left(1 + \frac{100}{S/N_o}\right) = (0.15)^2 \text{ chips}^2; \qquad N = 1, 2 \tag{4}$$

which describes the variance (Reference 2) of a code loop of bandwidth B_L in terms of signal-to-noise (S/N_o) (both in Hz) with an IF bandwidth of 50 Hz (data rate). N is the number of simultaneous measurements and is the number of correlators used for the code loop tracking.

The relationship of B_L T_T to S/N_o for a threshold condition of σN2 = (0.15)2 is presented in Figure 7 where T_T is tracking time per satellite. This figure coupled with the transient responses presented in Figures 8 through 10 express the relative benefit of first and second order code loops for a range of operating conditions. These responses are normalized to the aiding errors that might prevail, namely, the preposition code loop error σ_o, the aid frequency error δf (due to velocity) and the aiding frequency rate error δf (due to acceleration). Also shown is the benefit of using carrier loop aiding, disregarding the noise errors discussed earlier.

Note that for a second order loop to be of benefit, normalized times of B_L T_T of over, sa 1.5 are necessary to reduce the effect of velocity and acceleration errors. However, as shown in Figure 7, B_L T_T must be smaller than that to achieve low S/N thresholds. This requires accurate IGS aiding and eliminates any advantage of a higher order code loop.

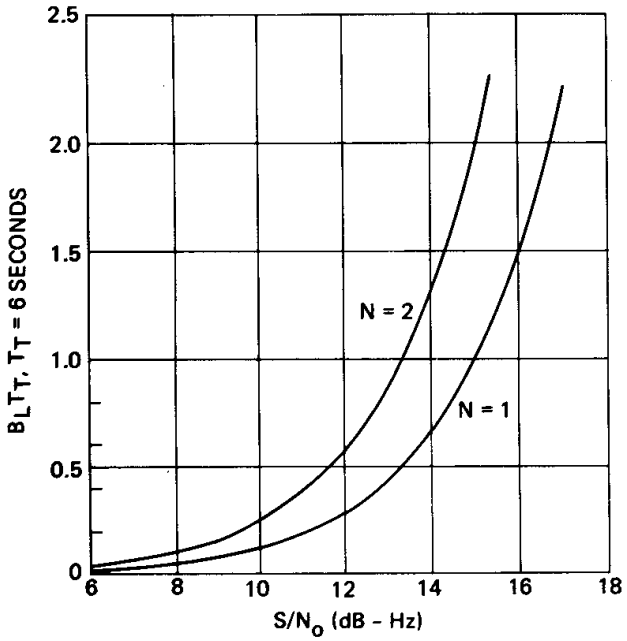

Fig. 7. Threshold B_L T_T versus signal-to-noise ($\sigma_n^2 = 0.15)^2$)

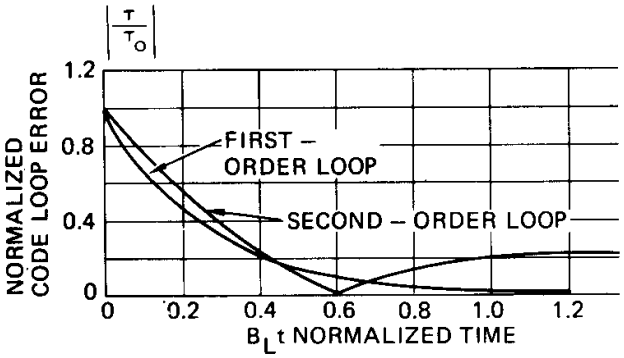

Fig. 8. Response of code loop due to initial code loop error

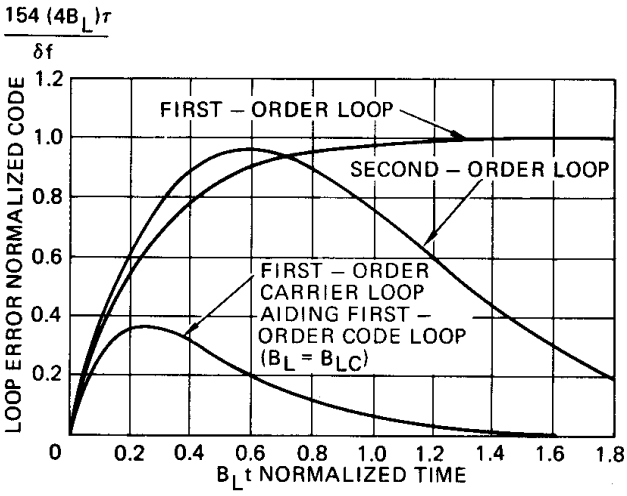

Fig. 9. Response of code loop due to constant frequency errors

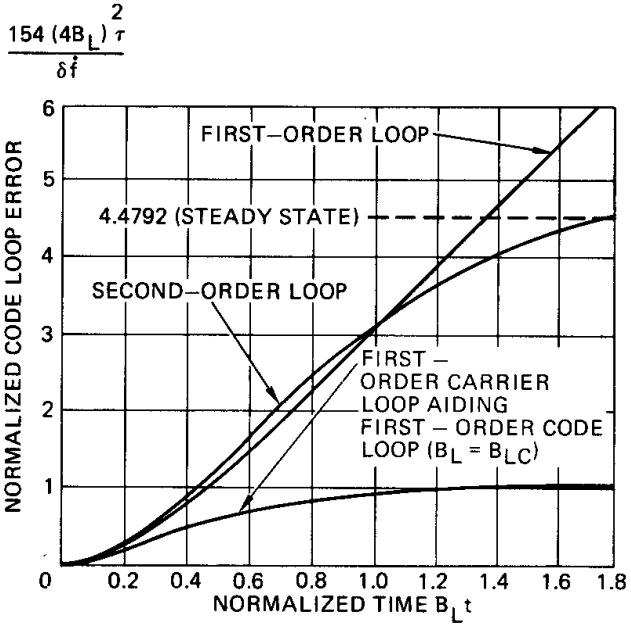

Fig. 10. Response to code loops due to constant acceleration errors

BANDWIDTH OPTIMIZATION

For the sequential tracking receiver (first order loop), the total measurement error variance is

$$\sigma^2_m = \frac{B_L}{N\ S/N_o}\left(1 + \frac{100}{S/N_o}\right) + \left(\sigma_{m_L}^2 + 9T^2_T\delta v^2\right) e^{-8B_L T_T} + \frac{(\delta v)^2}{16B_L^2}\left(1 - e^{-4B_L T_T}\right)^2 \quad (5)$$

for an IF bandwidth of 50 Hz, a tracking time T_T, a velocity aiding error δv (in chips per second) and a non-tracking time of 3 T_T. The value of N is either 1 or 2 equaling the number of correlators. The initial code loop error variance for the pull-in (second term) was selected to be the sum of the expected measurement variance σ_{mL}^2 (from the last measurement) plus the integrated effect of the velocity aiding error since the last measurement. ($9T_T^{2\delta v2}$ - 2 6v2). To optimize the bandwidth, equation 3 was minimized with respect to B_L by setting the partial derivative equal to zero.

The measurement errors after optimization are shown in Figure 11 for N = 1 (τ-dither) and N = 2 (simultaneous E/L) for a range of signal-to-noise ratios. These results were used as a basis for simultaneous whose results will be presented later.

ADAPTIVE BANDWIDTH

The bandwidth optimization presented above is for the selection of the bandwidth at the receiver's threshold, defining its ultimate J/S capability. It is desirable, however, to increase the bandwidth at higher signal-to-noise ratios in order to improve signal pull-in, and to withstand larget dynamic errors. An approach would be to increase the bandwidth as a function of estimated S/N_o. However, the M-receiver does it naturally, without estimating S/N_o because of the interaction with the code tracking loop and the Automatic Gain Control (AGC).

The AGC maintains a constant average total wideband power (P_o), in the in-phase, quadraphase measurement process. Thus, any decrease in the noise (or signal) power increases the AGC gain, which directly increases the code loop gain, and thus, its bandwidth. That variation of its bandwidth B_L is shown in Figure 12 as a function of the

increase (in dB) of the signal-to-noise (S/N_o) over the threshold signal-to-noise (S/N_{OTH}), as a ratio to the threshold bandwidth B_{LTH}.

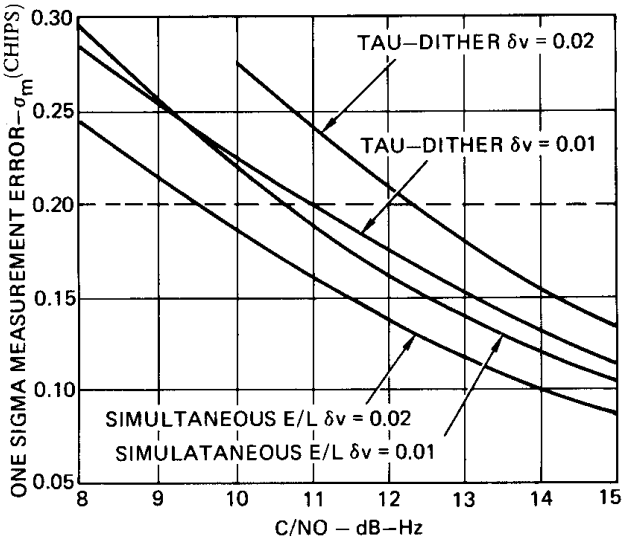

Fig. 11 Sequential tracking receiver code loop measurement performance

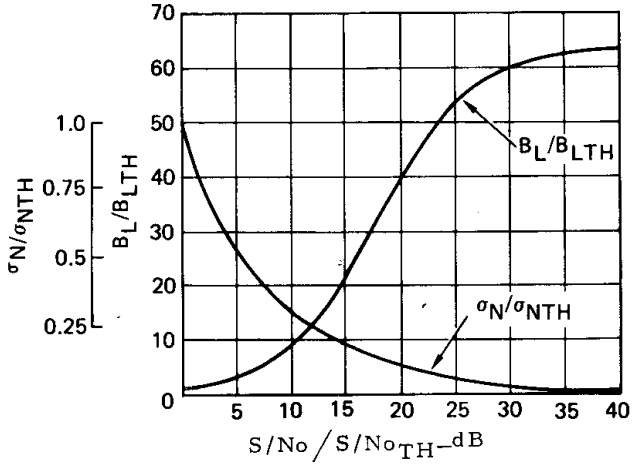

Fig. 12. Bandwidth adaptation to N/N_o and their effect on noise variance

Although the bandwidth of the code tracking loop increases with signal-to-noise, the noise variance does not stay at a near threshold level but decreases considerably. The ratio of one sigma noise to that of the threshold value is also plotted in Figure 12. The reasons for the decrease are two-fold. At high noise conditions, the decrease is due to the increase in squaring loss. At higher signal-to-noise conditions, it is due to the leveling off of the bandwidth because of the dominance of signal power on the AGC.

On the other hand, the IF (pre-detection) bandwidth is not self-adaptive to the noise. But then, its value is more sensitive to the frequency error rather than to the noise and it has a lower bound of 50 Hz because of the mostly unknown data stream on the incoming signal. It's effect on code loop performance at high J/S conditions, disregarding frequency errors, is the squaring loss in the power measurements, because the noise variance is (5).

$$\sigma_N^2 = \frac{B_L}{S/N_o}\left(1 + \frac{2B_{IF}}{S/N_o}\right) \qquad (6)$$

The second term in the parenthesis represents the squaring loss. Because B_{IF} has a lower bound, any adaptation in its value is only significant at higher signal-to-noise ratios, when power loss could be experienced due to relatively large frequency offsets, caused by a misaligned INS or unestimated clock frequency. In these situations, the receiver would be required to search and reacquire the signal due to large frequency errors. The M-Receiver/

Guidance Processor combination does adapt the IF bandwidth. However, it adapts on the basis of the Guidance Processor's estimate of the frequency error. This procedure is part of signal reacquisition.

SIGNAL REACQUISITION

Signal reacquisition might be required after launch when the receiver is switched over to the missile's antenna, or due to loss of lock because of a short period of extremely high jamming. In any event, the result would be a preposition or frequency error that would require the receiver to search out the signal. The receiver's decision to do so is based on the pre-position uncertainties provided it by the Guidance Processor — namely pseudorange (σ_{PR}) and pseudorange rate ($\sigma_{\Delta f}$) uncertainties.

THE FAST SEARCH

The primary purpose of the fast search (1000 Hz bandwidth) is for initial signal acquisition. For an IGS to have errors of the magnitude to require the fast search otherwise is highly unlikely. This search is used primarily for searching out initial time and frequency uncertain ties of the clock and local oscillator. It is this search that determines the TGPSG system's time-to-first-fix (TTFF).

THE MEDIUM SEARCH

The medium search (250 Hz bandwidth) is "the" primary reacquisition search. The limits on this medium search are a one sigma frequency uncertainty of 60 Hz and a one sigma pseudorange uncertainty of 20 P code chips. The 60 Hz one sigma frequency uncertainty is an estimate of the tolerable frequency error that will maintain a 0.95 Probability of Detection (P_D) with the 250 Hz predetection bandwidth, assuming a Gaussian distribution of frequency error. The Probability of Detection versus frequency for that bandwidth at 40 dB J/S for the M-Receiver detection algorithm is shown in Figure 13. The 60 Hz frequency uncertainty is equivalent to about 11 meters/sec line-of-sight velocity error, which is indeed a large error for an IGS. However, the capability to detect at this one sigma error at 40 dB J/S enhances the J/S capability of the M-Receiver.

THE SLOW SEARCH

The slow search (50 Hz bandwidth) is an added feature of the M-Receiver. It's primary purpose is to reacquire the satellite signals at a fairly high J/S, which is made possible by the relatively small uncertainties that can be maintained by the IGS over reasonable lengths of time, once it has been aligned. The frequency uncertainty limitation is 12 Hz based on the same reasoning presented for the 250 Hz search above. The 1.0 chip pseudorange

uncertainty is based on a time limitation dictated by the 6 second sequencing time, because a long period on signal is required to cope with the high JIS conditions.

Unlike the fast and medium search algorithms which use AGC controlled square law power measurements, the slow search algorithm uses a “normalized” hard limited power measurement (PH). This measurement is of the form

$$PH = \sum_{k=1}^{5} \left(\frac{I_k}{\sqrt{I_k^2 + Q_k^2}} \right)^2 + \sum_{k=1}^{5} \left(\frac{Q_k}{\sqrt{I_k^2 + Q_k^2}} \right)^2 \qquad (7)$$

where the I_k and Q_k are the in-phase and quadraphase components integrated over a 4 millisecond interval. The total measurement spans a 20 millisecond interval. The denominator is closely approximated with

$$\sqrt{I_k^2 + Q_k^2} = [0.9475 \max(|I_k|, |Q_k|) + 0.3925 \min(|I_k|, |Q_k|)] \qquad (8)$$

to simplify computations.

The advantage of the PH measurement of equation 7 over the square law power measurements is that it is normalized and is independent of AGC, and independent of signal-to-noise ratio variations. Being independent of signal-to-noise ratio variations makes it effective against modulating jammers or against signal variations due to changes in antenna patterns, etc. There is theoretically a loss of about 1.5 dB, with respect to the square law power uncertainties and quantization in the Automatic Gain Control.

As stated earlier, detection of a signal in noise is usually more difficult than tracking the signal once it is detected. This is also the case with the slow search detector. Figure 14 presents the performance of the slow search detector relative to the tracking threshold of the sequencing M-Receiver for two different search times, 4 and 6 seconds. The shaded area envelopes a variety of simulation results — simulations run with different false alarm rates and simulations run with and without the modelling of possible I and Q (in phase and quadraphase components) biases. The circled regions signify the relative J/S detection capabilities for a 0.9 Probability of Detection.

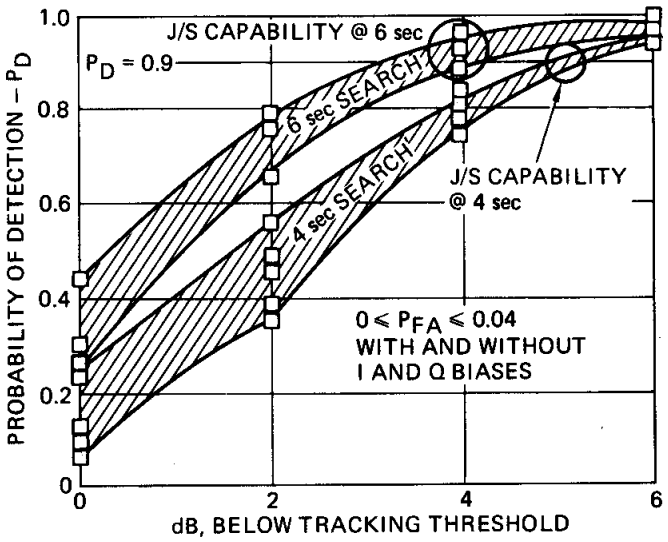

Fig. 14. Slow search detector simulation result

LOCK INDICATORS

To this point we have covered M-Receiver, acquisition, tracking and reacquisition of the satellite signals. However there is an important factor that is overlooked many times when the capabilities of receivers are stated, either as a requirement or as an advertised capability. That is, even though the receiver is capable of tracking a signal in a hostile environment with a high probability of success, how is it known that it is truly tracking that signal? The fact is that, like the case of acquiring a signal, it is usually more difficult to sense the presence of a signal than it is to track that signal. This is especially true with a sequencing receiver, for it has only a finite period of time to sense the presence. A continuously tracking receiver can absorb much more data before it makes its decision; however, the longer it takes, the more difficult it is to reacquire if it is lost.

The technique for sensing the presence of a signal is called a “lock indicator” here, and is much like a detector used while searching in an acquisition or reacquisition mode. The only difference is that the search takes place only in the position the signal is thought to be.

Lock indicators at higher signal-to-noise ratios, when carrier tracking is being performed, are relatively reliable and easy to implement. They are “AFC Lock” or “Costas Lock” indicators. In other words, they sense carrier tracking of one form or another at these higher signal-to-noise ratios. The more difficult indicator is that which detects and indicates lock at the very high J/S conditions when there is no carrier tracking — only an aided code loop when it is tracking at its threshold condition.

CODE LOOP LOCK INDICATOR

The lock indicator measurements during aided code loop operation take on the same form as those used in the slow search detector as described in equation 6. Because the same gain variation and C/N_o variation conditions could exist while tracking as during search. However, a problem unique to detection during tracking is, if tracking errors are small and both correlators are being used for the code tracking loop, measurements are being taken 6 dB below peak power (for ±1/2 chip differential power measurements). On the other hand, if tracking errors are large, e. g., 1/2 chip, half the measurements are being taken at peak power. Therefore, a compromise was made between an optimum tracking strategy and an optimum lock detection strategy. After trading various schemes for doing simultaneous tracking and lock detection, the following strategy was selected.

1. Perform simultaneous early and late power measurements using both correlators for code tracking, and integrate both early and late hard limited power (PH_E and PH_L for possible use in the lock indicator. Use this procedure for the first three seconds of the six second tracking interval to obtain the maximum signal pull-in.

2. After three seconds, use one correlator for tau-dithering (alternating early and late power measurements) for code tracking, and use the other correlator for "on-time" hard limited power measurements (PH_o) for use in the lock indicator. Initialize the integration of that "on-time" measurement with the maximum of the integration of the early and late measurements performed over the first three seconds. Use one-half the original bandwidth in the code tracking loop to maintain the results of the first three seconds.

3. At the end of six seconds, compare the output of the lock indicator integrator with a preselected threshold. An output above the threshold indicates that the signal is present.

This procedure is an attempt to supply the lock indicator with as much power as possible over the six second tracking interval. Even so, the performance of the indicator is marginal at the code tracking threshold.

CODE LOOP/LOCK INDICATOR SIMULATION

A code loop/lock indicator nonlinear simulation was developed that includes most of the effects of the M-Receiver's environment. These effects include jamming, rate-aiding and preposition errors and the sequencing operation. The simulation includes simulation of rate-aiding errors, generation of I's and Q's, code loop nonlinearities, effects of the rate-aiding errors on losses due to carrier frequency offsets, and the effects of AGC and the lock indicator. It does not simulate reacquisition nor carrier loop operations, as it was developed to simulate the receiver at its threshold at high J/S conditions.

SIMULATION RESULTS

Simulations were run over 40 to 50 sequencing cycles from initial preposition and rate-aiding errors to simulate a typical mission. The rate-aiding simulation was updated at each cycle with a Kalman filter (2 states) processing the simulated psuedorange measurement. The simulations were run at the threshold J/S condition.

Figure 15 represents a simulation output. The upper part of the figure is a plot of the simulated rate-aiding error in chips per second. The lower part of the figure is a plot of the pseudorange measurement errors superimposed on the preposition errors (dashed line) for that sequence that produced that measurement, both in chips. These errors agreed with the linearized analysis equations presented earlier.

Figure 16 presents the output of the lock indicator (integrator for each cycle corresponding to the tracking results of Figure 15). The simulation was repeated with the same set of random numbers with no signal and signal tracking. Outputs of both runs were plotted together to show the relationship of the probability of lock detection to the probability of false lock, and to the threshold of the lock indicator. Various threshold levels are indicated on the right hand side of the figure.

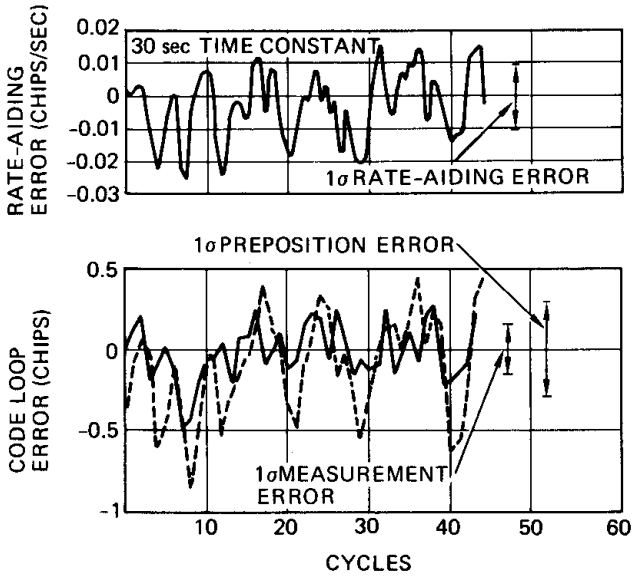

Fig. 15. Tracking results at threshold J/S conditions

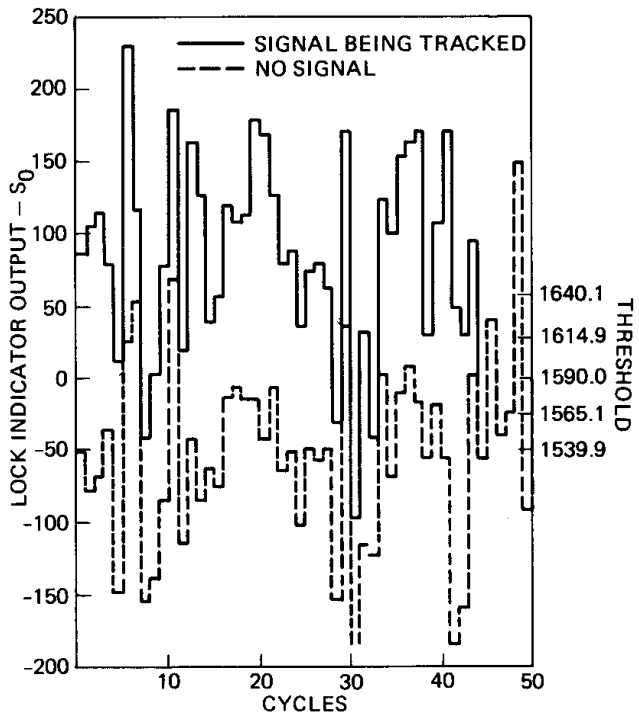

Fig. 16. Lock indicator output S_o

By varying the threshold, which can be done “a posteriori” the simulation, the relationship of false lock and detection probabilities can be determined. This relationship is plotted in Figure 17. They symbol (Δ) presents the results for using the results of one indication at a time. These results are somewhat marginal. However, if memory is built into the indicator (remembering the results of the last cycle), the overall lock indicator results can be improved significantly. That feature was built into the lock indicator.

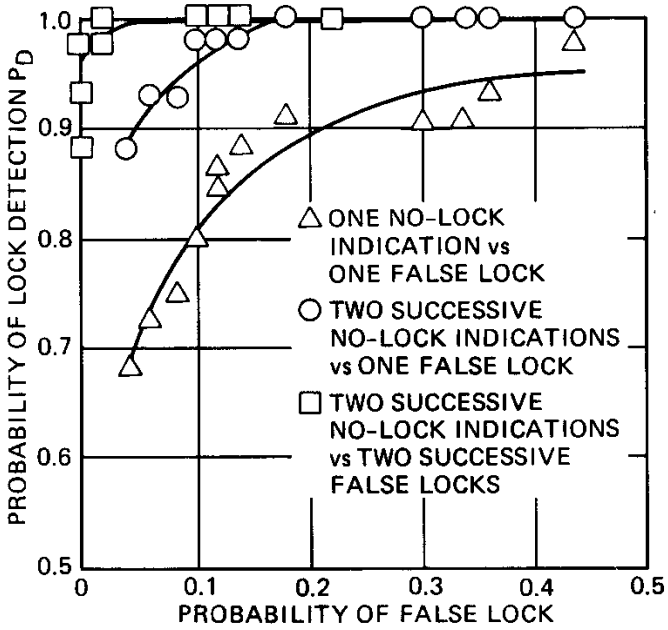

Fig. 17. Lock indicator results at threshold J/S conditions

The implications of using the lock indicator with memory is as follows:

1. Waiting for two “no lock” indications before declaring no lock delays a reacquisition of the signal by 24 seconds. If the IGS accuracy is of a magnitude to allow operation at this threshold J/S condition, waiting 24 seconds will not exceed the search capability of the slow search reacquisition mode. Because, if the threshold J/S condition exists, reacquisition would probably fail anyway.

2. A false lock could be interpreted to mean a delay in reacquisition given that the signal was being tracked and then lost, or it had never been acquired. Therefore, a false lock must always be coupled with the probability of a false acquisition or the probability of loss of signal (not loss of lock indication). Since the probability of either of these conditions should be quite low, the resulting probability of false lock during the course of a mission is very low, since it is that low probability times the probability of false lock given no signal.

Therefore, using a lock indicator with memory is justified as well as having acceptable performance.

The results of the simulation presented here verify the design and the performance of the M-Receiver. The same simulation was run with lower J/S conditions. In those cases, the performance improved significantly, as would be expected. In fact, the lock indicator output made the right decision with a high degree of success without memory. The improvement in tracking results verified that the tracking loop bandwidth adapted to signal-to-noise ratio.

NAVIGATION, FILTERING AND SIMULATION

The guidance system performance analysis effort had two primary goals; first, determining the performance of the operational system (TGPSG) and second, analyzing the flight test configuration of the system. The TGPSG system will consist of a strapped down inertial measurement unit (LCIGS) to provide vehicle acceleration and attitude, a sequential GPS receiver (M-receiver) and a digital computer (guidance processor - GP) for navigation, filtering and receiver aiding. The performance analysis addressed the question of navigation accuracy, receiver aiding accuracy and inertial instrument calibration. In the flight test program, a Litton LTN-51 inertial navigation system will be used for inertial measurements which provides a high quality, high reliability measurement system. The effects of LCIGS will be introduced by degrading the inertial measurements to LCIGS quality measurements in the guidance processor. A basic premise of the flight test program is that the LTN-51 errors are so small compared to those of the simulated LCIGS that they may be ignored when simulating the LCIGS.

NAVIGATION AND FILTER

In the TGPSG flight test system, the LTN-51 operates in normal fashion but its computer serves only to maintain the platform level. The LTN-51 operates open-loop with respect to the test system; that is, the system provides no information to the LTN-51. The outputs of the LTN-51 used by the guidance processor are the quantized outputs of the three accelerometers and three synchro outputs of vehicle attitude. The accelerometer outputs drive the inertial navigation computations. The vehicle attitude is used in simulating the system errors that would be caused by LCIGS and for antenna lever arm corrections.

The basic inertial navigation computation cycle time is one-tenth second. The quantized accelerometer outputs accumulated in each one-tenth second are corrected for the platform wander angle, the estimated misalignment of the platform, Coriolis accelerations and the local effective gravity to compute velocity and position with respect to the Earth. Inertia 1 navigation computations in the GP maintain North, West and up components for velocity,

and maintain geodetic latitude, longitude and altitude above the spheroid. The Earth spheroid and the Earth gravity model are those of WGS72, with the gravitational potential including only terms through J_2. The coordinate system chosen for inertial navigation is suitable only for use at the moderate latitudes at which system testing will be performed. Future systems with a strapped down inertial system may well require a navigation algorithm different from any that might have been selected at this time.

A Kalman filter will be used to estimate a 14 element navigation state vector on the basis of sequential measurements from four satellites. These elements are errors in latitude, longitude, altitude, velocity North, velocity West, velocity up, platform misalignment about the North, West and up axes, gyro drift about three orthogonal axes, and the receiver clock phase and frequency. When LCIGS simulation is not included, the estimated gyro drifts are about the LTN-51 platform axes; when LCIGS simulation is included, the estimated gyro drifts are about the aircraft body axes.

The U-D formulation of the Kalman filter is employed to avoid the necessity for double precision computations in the filter and to assure filter stability.

In the Kalman filter, it is necessary to find transition matrices to update state vector estimates and covariance matrices with time. These transition matrices are found by integrating the linearized equation for the state vector errors by means of the Peano-Baker method, using two iterations where necessary. This requires the summing of twenty-five simple expressions every tenth of a second, and computation of the transition matrix from these sums every six seconds.

The LCIGS will be simulated in the GP in the following fashion: The integrals of the acceleration components in each one-tenth second will be resolved through the wander angle and through the estimated misalignment angles to, North, West and up. They will then be resolved through the aircraft attitude angles to aircraft axis components. These components will then be used to calculate the simulated, acceleration-dependent, strapped down gyro and accelerometer errors. The included errors are gyro biases, gyro g-sensitive drifts, gyro g-squared-sensitive drifts, accelerometer biases and accelerometer misalignment and scale factor errors. The LCIGS simulated gyro drifts are accumulated. The one-tenth second integrals of acceleration in aircraft coordinates are modified according to the LCIGS errors and rotated back to North, West and up for use in the inertial navigation computations.

SIMULATION PROGRAM

A simulation program was written to test the inertial navigation and Kalman filter programs. This simulation allows the IMU actual position, velocity and attitude to be

specified at a number of instants of time, and smoothly interpolates between these instants, so that position, velocity and attitude vary smoothly with time. Acceleration and attitude rate may have discontinuites at the time at which position, velocity and attitude are specified.

The specified actual position, velocity and attitude are used by the simulation program to determine what the LTN-51 accelerometer readings would be and to simulate the sensor performance and the computing algorithm of the LTN-51, including the ΔV's that would be output to the GP.

The simulation program includes the flight test, real-time software as a subprogram, so that the GP inertial navigation algorithm may now be exercised. In addition, another part of the GP program is used to generate aiding signals for the M-receiver and the simulation program models the performance of the M-receiver, including the effects of imperfect aiding, jammer-to-signal ratio, ionospheric delay, M-receiver clock errors and the displacement between the IGS and its antenna.

In order to aid the M-receiver and to use the M-receiver measurements, the GP performs ephemeris computations for the four GPS satellites. It uses the actual vehicle position in order to determine what the noise-free measured values of the measurables will be, and adds an error corresponding ot the uncertainty in satellite orbit.

The GP may use either the pseudorange measurement or the pseudorange measurement and the pseudo-delta range measurement as Kalman filter inputs, depending on the quality of the data. If both measurements are used, they are processed sequentially as scalars, rather than as a single vector measurement, and their errors are assumed to be independent.

SIMULATION CONDITIONS

The basic flight path followed by the vehicle for the simulation results reported here is shown in Figure 18. During the entire flight, measurements are taken in cyclic order from four satellites, obtaining measurements and switching satellites at intervals of six seconds. During the first 180 seconds of flight the measurements from each satellite include both pseudorange and delta-pseudorange, obtained at the same times. For the remainder of each flight, only pseudorange measurements are used. The jammer-to-signal ratio starts at a low value in each flight and gradually increases; this is reflected in the measurements in the form of increasing noise.

The approximate azimuths and elevations of the four satellites with respect to the vehicle are shown in Figure 19. The actual azimuth and elevations are time varying, because of the

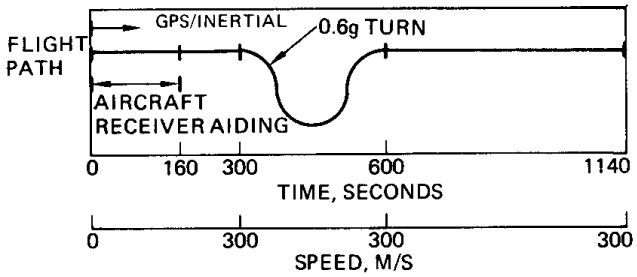

Fig. 18. Flight conditions for system alignment

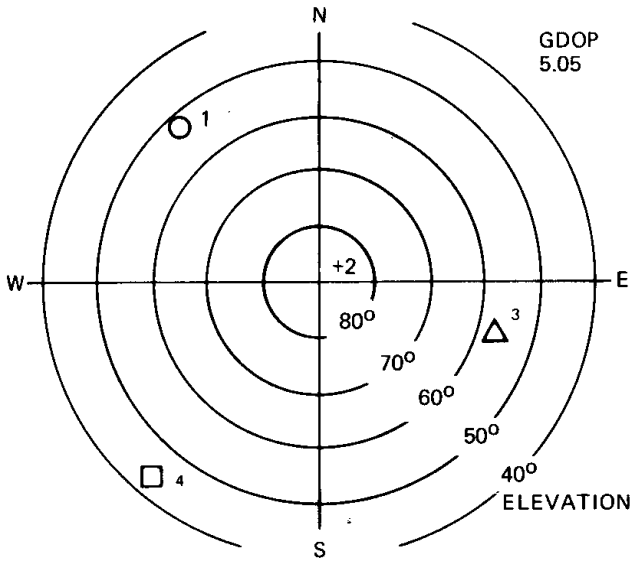

Fig. 19. Satellite local elevation and azimuth

motion of the satellites in their orbits, the rotation of the Earth and the motion of the vehicle with respect to the Earth. The configuration of the four satellites corresponds to a geometric dilution of precision (GDOP) of about 5. By way of comparison, an optimum distribution of satellites, with one at the zenith and the other three separated by 120 degrees at the horizon have a GDOP of 1.73.

Simulations were run both with and without LCIGS simulation being included. The runs without LCIGS simulation provides a standard of reference against which the results of the runs with LCIGS simulation can be compared. Three sets of runs are shown illustrating system performance of the system including LCIGS simulation with the system without LCIGS simulation. The second shows the effects of the loss of satellite measurements. The final set indicates what happens in a prolonged high-g maneuver. The assumed values of a priori covariance of the navigation state vector estimate and the process noise when LCIGS simulation is included are different from their assumed values when LCIGS simulation is not included, since the distributions of actual navigation state vector errors are different.

The first set of runs compares the results of four LCIGS simulation runs differing only in the measurement noise samples, with the results of similar runs with no LCIGS simulation. These comparisons show the effects of using a lower quality inertial measurements. The results appear in Figures 20 through 25. The RSS position errors, do not vary greatly between the LCIGS and non-LCIGS systems, depending primarily upon the GPS measurements - enough information is obtained from GPS measurements from 24 seconds to make a good estimate of position even with extremely large inertial measurement unit

(IMU) errors. Velocity errors are more dependent on IMU errors, so that the poorer performance of the LCIGS starts to become evident in Figure 22 even here the differences are not large. The differences in misalignment errors and drift rate errors are more evident.

The second set of runs is concerned with the effect of the loss of satellite measurements. The results of two of these runs are illustrated in Figure 26, corresponding to two different LCIGS systems having accelerometer biases of 200 and 1000 micro-g, respectively. The difference in system performance with accelerometer bias are quite evident in the figure, but there is no apparent effect on performance resulting from the loss of data from two satellites for a period of a minute. The effect of poorer quality measurements caused by increasing J/S can also be seen by comparing the velocity error at the earliest time shown with the velocity error at the latest time shown.

The last set of runs reported illustrate the effect of a prolonged high-g maneuver on the errors in the estimates of position and velocity. The 5-g turn begins 1040 seconds after the start of flight and persists for about sixty seconds. A turn of this duration and acceleration is highly unlikely, but serves to illustrate system performance. High-g turns are likely to be evasive maneuvers of short duration. Figures 27 and 28 show the position and velocity errors in three runs differing in the magnitude of the accelerometer bias. Whether the accelerometer bias is 100, 200 or 1000 micro-g, the turn results in similar errors in position and velocity , and within a short time after the end of the turn, the effects of the turn on the errors in position and velocity have disappeared.

1. Hardy, F. W. and Major C. D. DePriest, “Global Positioning System Tactical Missile Guidance,” AGARD Conference, Impact of Integrated Guidance and Control Technology on Weapon System Design, Norway, May 1978.

2. Kriegsman, B. A. , Cox, D. B. Jr. , Stonestreet, W. M., “An IMU-Aided GPS Receiver,” Presented at the 33rd Annual Meeting of the ION, Costa Mesa, CA, June 1977.

3. Chan, C. R. , “Threshold Reduction of a GPS Receiver by IMU Aiding,” Magnavox Report No. MX-TM-3175-75, 30 May 1975.

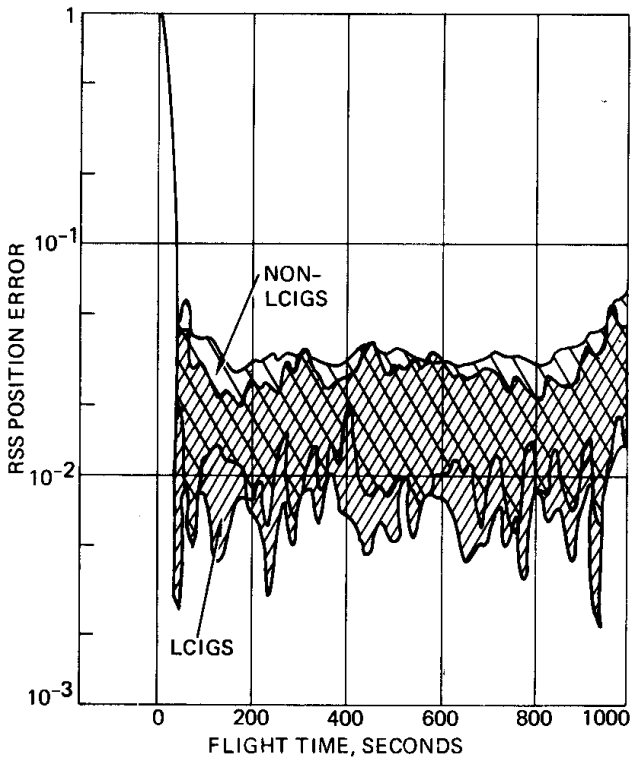

Fig. 20. Relative RSS position error

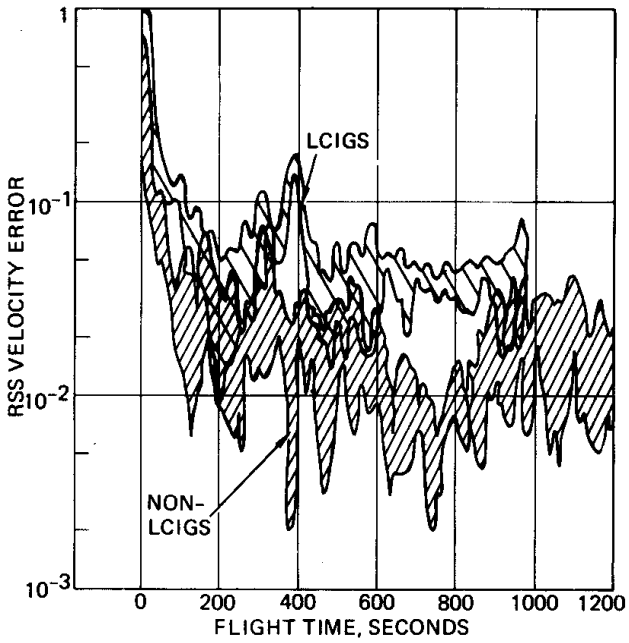

Fig. 21. Relative RSS velocity error

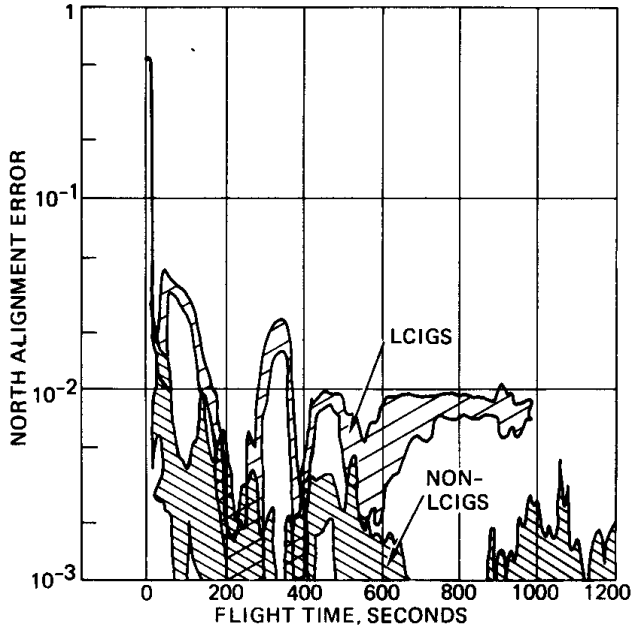

Fig. 22. Relative misalignment about north axis

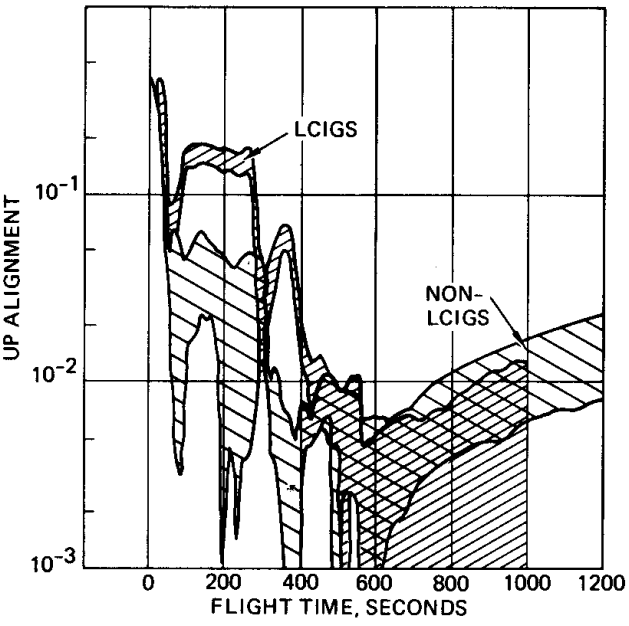

Fig. 23. Relative misalignment about up axis

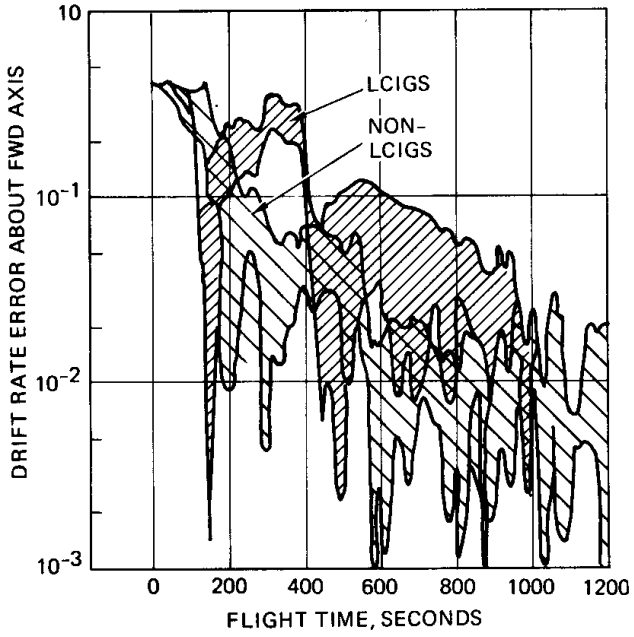

Fig. 24. Relative drift error about forward axis

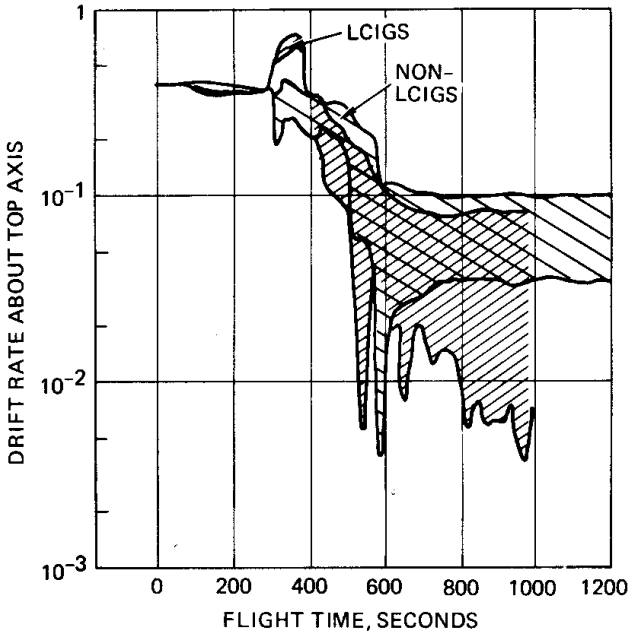

Fig. 25. Relative drift error about top axis

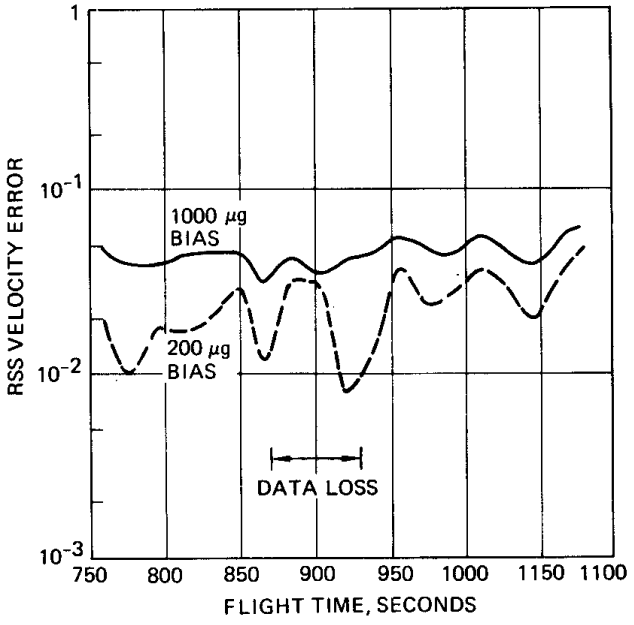

Fig. 26. Loss of data from Satellites 3 and 4 (LCIGS)

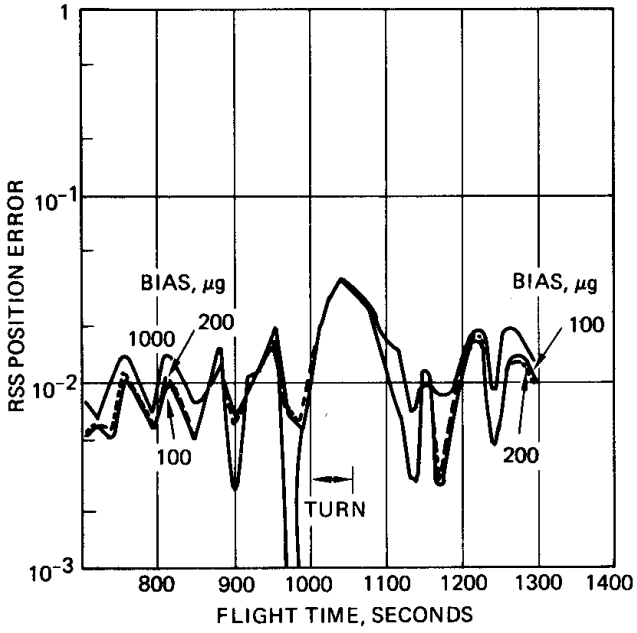

Fig. 27. Relative position error in 5-G turn

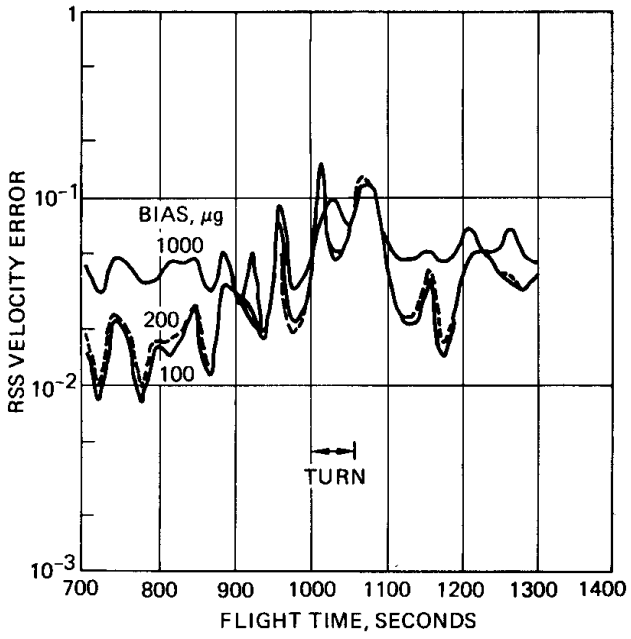

Fig. 28. Relative velocity in 5-G turn